Expansion Characteristics of Tapered Fluidized Beds

Renzo DiFelice, Piero U. Foscolo, Larry G. Gibilaro, Graham B. Wallis, and Renzo Carta
Dept. of Chemical and Biochemical Engineering, University College London, London WC1 7JE, UK

The effects of taper on the steady-state expansion characteristics of a homogeneous fluidized bed are examined theoretically and experimentally. It is shown that secondary factors that might be thought to influence the expansion (fluid accelerational effects including added mass and particle phase elasticity) are unlikely to be of significance in practical situations.

Introduction

This article concerns fluidization in a bed whose cross-sectional area varies continuously, either increasing or decreasing, with distance along the vertical axis. Experimental investigations have been previously reported for the case of an increasing taper, notably by Webster and Perona (1990) and Maruyama et al. (1984); however, a theoretical consideration of factors brought into play by the continuously changing fluid velocity in the bed does not appear to have been made, nor do there appear to have been any reported experiments on beds with a decreasing taper in which the fluid velocity increases with height. This latter omission is hardly surprising given the practical motivation for previous studies that sought to examine the potential for reduced fines carryover that could result in a bed in which fluid velocity progressively decreases and the increase in convective mixing that could be expected to occur where particle concentration, and hence bulk density, increase with height.

In what follows we restrict consideration to steady-state, homogeneous fluidization of essentially monosize, spherical particles. We employ a general formulation of the one-dimensional fluid and particle momentum equations that has proved successful in predicting dynamic phenomena, notably the onset of bubbling in fluidized beds (Foscolo et al., 1989). When this model is applied to steady-state operation in a normal bed, it yields the empirical result for homogeneous fluidization,

$$u_\infty/u_t = \epsilon^n, \tag{1}$$

first proposed by Richardson and Zaki (1954). This declares the entire bed to manifest void fraction ϵ when the fluid flux is u_∞; the empirical exponent n may be obtained from well established correlations requiring solely the particle Reynolds number under terminal conditions, $\mathrm{Re}_t = \rho u_t d_p/\mu$. This result in no way represents a prediction of the dynamic model, but merely reflects the incorporation of relation 1 into the general expression for fluid-particle drag that appears in the momentum equations.

When, as we shall see, the effect of a taper is incorporated in the continuity and momentum equations, the time invariable situation no longer conforms to the trivial law of Eq. 1. Mechanisms, which in a conventional bed affect only the dynamic behavior, now come into play and may be subjected to quantitative evaluation. They comprise the influence of fluid acceleration on the momentum flux in the bed and in promoting inertial coupling between the phases, as well as the effective particle-phase elasticity that contributes to the particle momentum equation when axial concentration gradients, absent in the equilibrium operation of conventional beds, occur.

Tapered Beds

Figure 1 shows side elevations of the circular cross-section beds considered in this study. Fluid enters through the distributor plate of diameter D_o. The relevant geometry of the bed is defined by this diameter and the vertical vector, of length z_o, from the distributor to the apex of the cone of which the bed forms a part. This convention, which defines z_o to be positive for decreasing tapers and negative for increasing tapers, leads to the following relationship between vertical distance and bed diameter for both cases:

$$D/D_o = 1 - z/z_o \tag{2}$$

Correspondence concerning this article should be addressed to L. G. Gibilaro. Present addresses of: R. Di Felice, Dipartimento di Chimica, Ingegneria Chimica e Materiale, Universita di L'Aquila, 67100, L' Aquila, Italy; G. B. Wallis, Thayer School of Engineering, Dartmouth College, Hanover, NH 03755; and R. Carta, Dipartimento di Ingegneria Chimica e dei Materiali, Universita di Cagliari, 09100, Cagliari, Italy.

The Particle Bed Model

The formulation of the equations of change for a fluidized suspension, that we later adapt to the case of equilibrium, tapered beds, is described by Foscolo et al. (1989). The equations of relevance for our present purpose describe conservation of mass for the fluid phase,

$$\partial\epsilon/\partial t + \partial[\epsilon u_f]/\partial z = 0 \tag{3}$$

and the combined momentum equation for both fluid and particle phases,

$$\rho_f Du_f/Dt - \rho_p\, Du_p/Dt = (\rho_p - \rho_f)g - F_D/[(1-\epsilon)\epsilon] - E_p/(1-\epsilon)\partial\epsilon/\partial z \tag{4}$$

Equation 4 was obtained from the individual fluid and particle momentum conservation equations following the general procedure of Wallis (1969), which involves elimination of the fluid pressure gradient term that appears in each. Constitutive expressions for drag force F_D and particle phase elasticity E_p close these equations. Under equilibrium conditions, Eq. 4 reduces to Eq. 1.

Equations of Change for Equilibrium, Tapered Fluidized Beds

The equilibrium state is characterized by a stationary particle phase, $u_p = 0$. The control volume is bounded by a circular cross-section of bed whose diameter changes with axial distance in accordance with Eq. 2. On this basis, the conservation equations are readily formulated as follows.

Fluid-phase continuity

$$\frac{d}{dz}(D^2 u_f \epsilon) = 0, \tag{5}$$

which, on expansion and application of Eq. 2, yields:

$$\frac{du_f}{dz} = -u_f\left[\frac{1}{\epsilon}\frac{d\epsilon}{dz} - \frac{2}{z_0 - z}\right]. \tag{6}$$

u_f may be related to the flux, u_∞, at the distributor plate through

$$D^2 \epsilon u_f = D_0^2 u_\infty, \tag{7}$$

which, together with Eq. 2, yields:

$$u_f = \left(\frac{z_0}{z_0 - z}\right)^2 \frac{u_\infty}{\epsilon} \tag{8}$$

Momentum equations

For the particle phase, we may write:

$$-(1-\epsilon)\rho_p g - (1-\epsilon)\frac{dp_f}{dz} + F_D + E_p\frac{d\epsilon}{dz} = 0 \tag{9}$$

These terms represent the actions on the particle phase in a control volume of gravity, effective buoyancy, fluid-particle drag and particle-phase elasticity, respectively. The drag force F_D, expressed in terms of the fluid flux u_∞ at the distributor plate, becomes:

$$F_D = (1-\epsilon)(\rho_p - \rho_f)g\left[\left(\frac{z_0}{z_0 - z}\right)^2 \frac{u_\infty}{u_t}\right]^{4.8/n} \epsilon^{-3.8}. \tag{10}$$

The particle-phase compressibility arises from hydrodynamic forces. When small perturbations about equilibrium are involved, the elasticity modulus E_p reduces to (Foscolo and Gibilaro, 1987):

$$E_p = 3.2(1-\epsilon)g d_p(\rho_p - \rho_f), \tag{11}$$

which is the same term that applies to cylindrical beds.

For the fluid phase, we have:

$$\epsilon\rho_f u_f \frac{du_f}{dz} + \epsilon\rho_f g + F_D + \epsilon\frac{dp_f}{dz} = 0. \tag{12}$$

The last term in Eq. 12 represents the sum of the buoyant reaction from the particles and the surface forces acting across the control volume boundaries.

The equilibrium counterpart of the combined momentum equation, Eq. 4, for a tapered bed may now be obtained on elimination of dp_f/dz in Eqs. 9 and 12.

$$\rho_f u_f \frac{du_f}{dz} + \frac{E_p}{1-\epsilon}\frac{d\epsilon}{dz} = (\rho_p - \rho_f)g - \frac{F_D}{\epsilon(1-\epsilon)}. \tag{13}$$

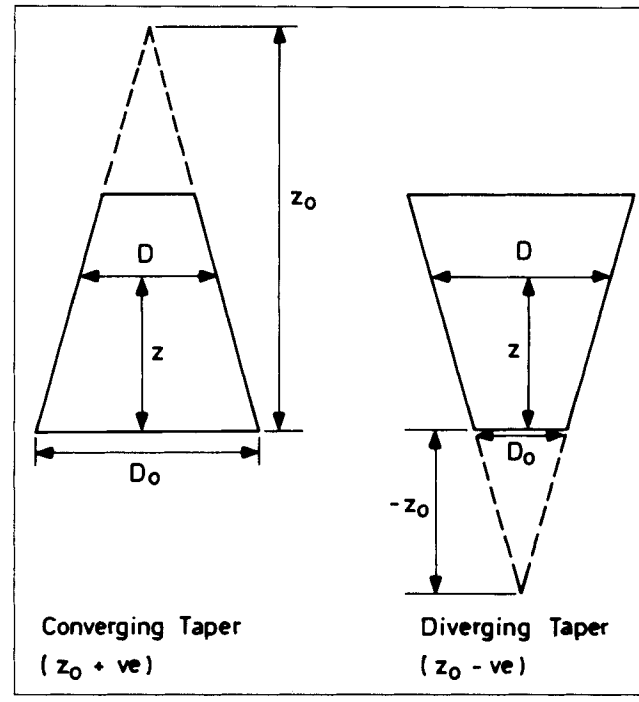

Figure 1. Side elevations of the circulation cross-section tapered beds.

Void Fraction Profile

Substitution of du_f/dz and u_f in Eq. 13 from Eqs. 6 and 8 yields the differential equation describing the equilibrium void fraction profile $\epsilon(z)$ in the tapered bed:

$$\frac{d\epsilon}{dz}=\frac{(P+Q)}{(R-S)}, \tag{14}$$

where the terms on the righthand side take the following forms:

$$P=(\rho_p-\rho_f)g\left[\left(\frac{z_0^2}{(z_0-z)^2}\frac{u_\infty}{u_t}\right)^{4.8/n}\epsilon^{-4.8}-1\right]; \tag{15}$$

$$Q=2\rho_f\frac{u_\infty^2}{\epsilon^2}\frac{z_0^4}{(z_0-z)^5}; \tag{16}$$

$$R=\rho_f\left(\frac{z_0}{z_0-z}\right)^4\frac{u_\infty^2}{\epsilon^3}; \tag{17}$$

$$S=3.2gd_p(\rho_p-\rho_f). \tag{18}$$

The significance of each of these terms may be readily identified: P represents the net effect of gravity, fluid-particle drag and buoyancy, these being the only effects felt in a conventional cylindrical bed; Q and R represent the effects of the taper and the void fraction gradient on the momentum of the fluid, respectively; and S represents the effect of particle-phase elasticity, that is attributed, in the model formulation employed here (Foscolo and Gibilaro, 1987), to fluid dynamic interactions.

In addition to the above effects, we must consider inertial coupling or "added mass" that occurs where there is relative acceleration between phases. Wallis (1990) has shown that for the combined momentum equation formulation employed above, this effect can be well approximated by the simple expedient of augmenting fluid and particle densities, wherever they occur, by $\rho_f/2$. This affects the fluid acceleration terms Q and R in Eq. 14, thereby enabling the influence of added mass on the void fraction profile to be assessed.

Simple Model Solution

In the next section, we assess the relative importance of the terms in Eq. 4 for practically realizable situations. In the meantime, however, we can, by ignoring fluid acceleration and particle-phase elasticity effects (by setting Q, R, and S to zero), obtain the trivial solution to Eq. 4 that corresponds to a cylindrical bed where drag and buoyancy alone support the weight of the particle phase. On this basis, Eq. 4 reduces to

$$P=0,$$

which yields:

$$\epsilon=\epsilon_{RZ}=\left[\left(\frac{z_0}{z_0-z}\right)^2\frac{u_\infty}{u_t}\right]^{1/n}. \tag{20}$$

For a cylindrical bed, $z_0\to\pm\infty$, Eq. 20 reduces to the Richardson-Zaki expression, Eq. 1.

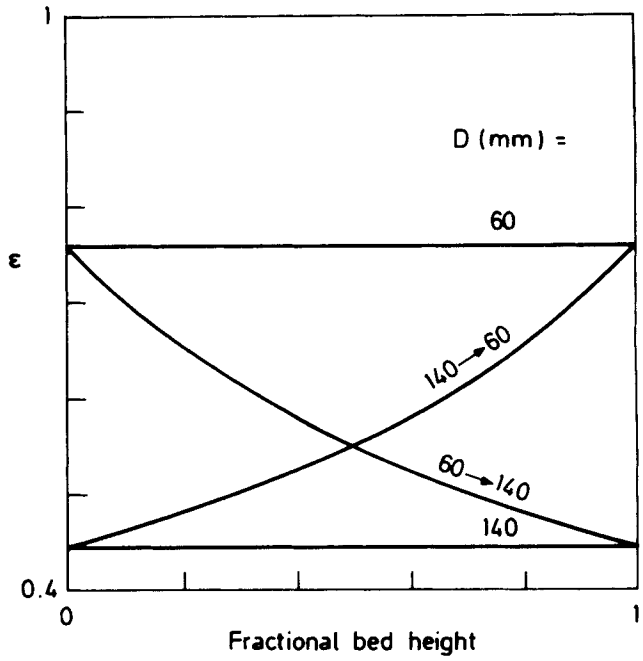

Figure 2. Void fraction profiles in tapered beds.

Solutions to Eq. 14 for water fluidization of 0.425-mm lead glass spheres; flow rate, $10^{-4}m^3\cdot s^{-1}$.

Numerical Predictions

Equation 14, with the terms defined by eqs. 15–18, provides a fully predictive basis for evaluating the equilibrium expansion, characteristics of tapered fluidized beds. The only empirical inputs, u_t and n, are readily available either from well established correlations or, better, from direct measurements carried out in a conventional cylindrical bed using the relevant fluid and particles. The volumetric flux at the distributor u_∞ is obtained from the volumetric flow rate q:

$$u_\infty=4q/\pi D_0^2. \tag{21}$$

The extent of taper is limited in practice by the requirement that the whole bed is to be in the fluidized state: the fluid velocity at the narrowest point must be substantially below u_t and, at the widest point, above that required to achieve minimum fluidization conditions. With this in mind, the simulations and experimental results we report below have been obtained for the case of a bed 900 mm in length with end diameters of 60 mm and 140 mm. When used as a diverging bed, the characteristic dimensions are (see Figure 1) $D_0=60$ mm and $z_0=-675$ mm; for the converging orientation, these become $D_0=140$ mm and $z_0=1575$ mm.

The solutions to Eq. 14 were obtained by an iterative method using, for the first estimate of bed concentration profile $\epsilon(z)$ Eq. 20, which ignores all secondary effects. A standard collocation routine also proved satisfactory for obtaining numerical solutions, but marching methods, tried initially, proved very unstable and were abandoned.

A wide variety of both liquid- and gas-fluidized systems, including those for which the implicit assumption of homogeneous fluidization was clearly invalid, were examined and found to correspond to the specific solutions we now report with regard to the relative importance of the various effects.

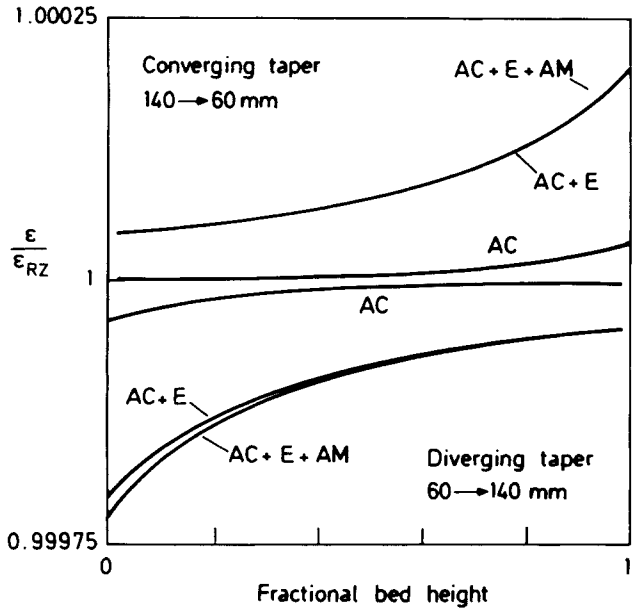

Figure 3. Effect of fluid acceleration, particle-phase elasticity and "added mass" on void fraction profiles in tapered beds.

Same system as for Figure 2.

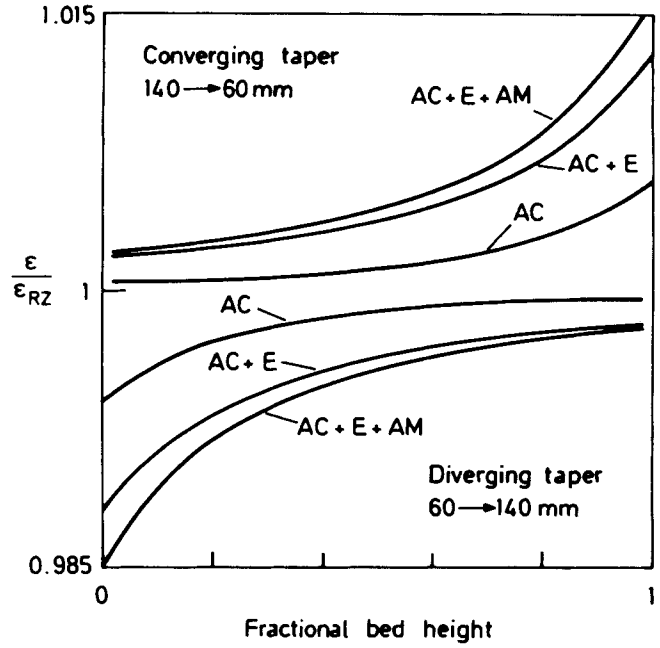

Figure 4. Effect of fluid acceleration, particle-phase elasticity, and "added mass" on void fraction profiles in tapered beds.

Water fluidization of 10-mm lead glass spheres; flow rate, $1.33 \times 10^{-3} m^3 s^{-1}$; bed geometry as indicated in Figure 2.

Figure 2 shows solutions to Eq. 14 for water fluidization of glass spheres in the tapered beds described above, together with those for cylindrical beds corresponding to the extreme diameter values. The significance of various effects are shown in Figure 3 as a consequence of the taper. The results are presented as the ratio of the void fraction, where one or more taper effects are included, to the void fraction ϵ_{RZ} (Eq. 20), where only drag, buoyancy and gravity are considered. The symbols *AC*, *E* and *AM* refer to inclusion of effects due to acceleration of the fluid (terms *Q* and *R*), particle-phase elasticity (term *S*), and "added mass" (included as described above), respectively. It will be seen from Figure 3 that, for this typical water fluidization example, particle-phase elasticity represents the major effect due to the taper, but that even this contribution is quite negligible from a practical point of view.

A more extreme example is illustrated in Figure 4. However, even for this case, which well exceeds the boundaries of homogeneous fluidization (Gibilaro et al., 1986), very little influence is felt from factors brought into play by the effect of the taper.

Experimental Study

A tapered bed, corresponding to the dimensions given above, was produced by machining a tapered hole through a $900 \times 150 \times 150$-mm block of perspex. It was inserted, in both the converging and diverging taper orientations, in the liquid fluidization rig, provided with a sintered metal distributor plate, described by Di Felice et al. (1987); the bottom few centimeters of bed was packed with lead shot to provide a more uniform liquid distribution.

Expansion characteristics for glass-water systems are reported in Figure 5. These broadly follow the predictions which, on the scale shown, cannot distinguish between the full solution of Eq. 14 and the simple expression of Eq. 20.

Discussion

At first sight, it is perhaps surprising that the taper parameter z_0 does not appear explicitly in the momentum equations (Eqs. 9, 12 and 13), except in the drag force term F_D (Eq. 10) and through the fluid velocity (Eqs. 6 and 8) and pressure gradient

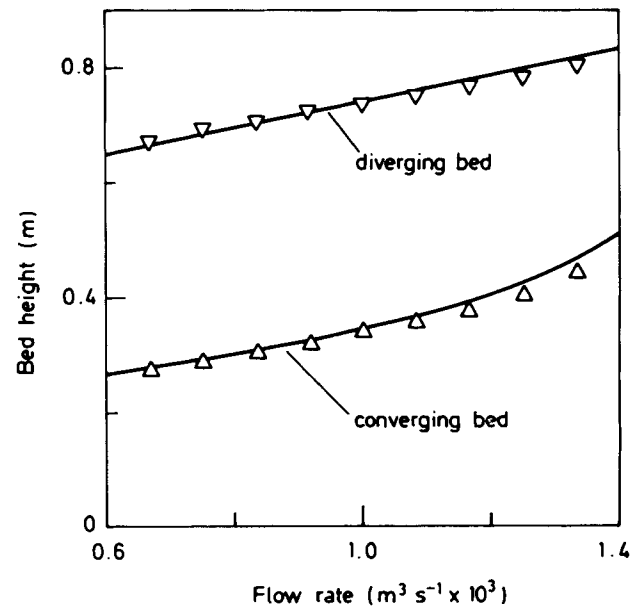

Figure 5. Expansion characteristics of tapered fluidized beds.

Comparison of experimental measurements (points) with model predictions (continuous lines); system, 4 kg of water fluidization of 4-mm soda glass spheres.

relationships. This is because its contribution to the fluid momentum flux disappears on application of the continuity relationship, fluid pressure gradient effects either derive from buoyant reactions within the control volume or (when attributable to forces at the control volume boundaries) include wall reactions in the axial direction, and the particle-phase elasticity term is evaluated, by consideration of void fraction perturbations about the equilibrium state, as previously described (Foscolo and Gibilaro, 1987).

Solutions to the derived void fraction dependence on axial distance along a tapered bed, Eq. 14, enable the direct effects of the taper to be investigated for any system of interest. A comprehensive examination of feasible liquid- and gas-fluidized situations failed to record significant departures in equilibrium behavior from predictions, Eq. 20, that ignore all contributions of fluid acceleration and particle-phase elasticity. The results reported above are typical in this respect. They also show that, of all these direct effects, particle-phase elasticity is the strongest and depends effectively on particle size alone. This last point can be verified by ignoring the less significant fluid accelerational contributions to Eq. 14 by settling $Q=R=O$; this has the effect of making the voidage gradient largely independent of particle-fluid density difference and inversely proportional to particle diameter—a result that was confirmed by the numerical solutions to Eq. 14.

Another effect of a taper could be to influence axial mixing of both fluid and particle phases. As mentioned earlier, this has been the focus of earlier experimental investigations into diverging taped beds that confirmed increased axial mixing due presumably to instabilities resulting from having the highest bulk density suspension at the top of the bed. Conversely one might expect reduced axial mixing in converging tapered systems. As it is unclear how mixing could effect equilibrium void fraction profiles, it was felt that converging taper systems could be more successful in studying the effects dealt with above. Upward movement of particles at the wall was observed for cases of converging taper, with downward wall flow for diverging cases. The expansion characteristics, Figure 5, however, which could be expected to average out local sampling inconsistencies, all showed good agreement with the model.

Notation

d_p = particle diameter, m
D = bed diameter, m
D_o = distributor diameter, m
E_p = particle phase elastic modulus, N/m^2
F_D = fluid-particle drag force, N/m^3
g = gravitational field strength, N/kg
n = exponent in Eq. 1
P = defined by Eq. 15, N/m^3
p_f = fluid pressure, N/m^2
q = volumetric liquid flow rate, m^3/s
Q = defined by Eq. 16, N/m^3
R = defined by Eq. 17, N/m^2
Re_t = terminal particle Reynold's number
S = defined by Eq. 18, N/m^2
t = time, s
u_f = fluid velocity, m/s
u_p = particle velocity, m/s
u_t = terminal particle settling velocity, m/s
u_∞ = volumetric fluid flux at distributor, m/s
z = axial distance, m
z_0 = defined in Figure 1, m

Greek letters

ϵ = void fraction
ϵ_{RZ} = defined by Eq. 20
μ = fluid viscosity, $N \cdot s/m^2$
ρ_f = particle density, kg/m^3
ρ_p = particle density, kg/m^3

Literature Cited

Di Felice, R., L. G. Gibilaro, S. P. Waldram, and P. U. Foscolo, "Mixing and Segregation of Binary-Solid Liquid Fluidized Beds," *Chem. Eng. Sci.*, **42**, 639 (1987).

Foscolo, P. U., and L. G. Gibilaro, "Fluid Dynamic Stability of Fluidized Suspensions," *Chem. Eng. Sci.*, **42**, 1489 (1987).

Foscolo, P. U., R. Di Felice, and L. G. Gibilaro, "The Pressure Field in an Unsteady-State Fluidized Bed," *AIChE J.*, **35**, 1921 (1989).

Gibilaro, L. G., I. Hossain, and P. U. Foscolo, "Aggregate Behavior of Liquid Fluidized Beds," *Can. J. of Chem. Eng.*, **64**, 931 (1986).

Maruyama, T., H. Maeda, and T. Mizushina, "Liquid Fluidization in Tapered Beds," *J. of Chem. Eng. of Japan.*, **17**, 132 (1984).

Richardson, J. F., and W. N. Zaki, "Sedimentation and Fluidization: 1," *Trans. Instn. Chem. Engrs.*, **32**, 35 (1954).

Wallis, G. B., *One-Dimensional Two-Phase Flow*, McGraw-Hill, New York (1969).

Wallis, G. B., "On Geurst's Equations for Inertial Coupling in Two-Phase Flow," *Two-Phase Flows and Waves*, D. D. Joseph and D. G. Schaeffer, eds., Springer-Verlag, New York (1990).

Webster, G. H., and J. J. Perona, "The Effect of Taper Angle on the Hydrodynamics of a Tapered Liquid-Solid Fluidized Bed," *AIChE Symp. Ser. Advances in Fluidization Engineering*, **86**(276), 104 (1990).

Manuscript received May 10, 1991, and revision received July 17, 1991.